Distribution Agreement

In presenting this thesis as a partial fulfillment of the requirements for a degree from Emory University, I hereby grant to Emory University and its agents the non-exclusive license to archive, make accessible, and display my thesis in whole or in part in all forms of media, now or hereafter now, including display on the World Wide Web. I understand that I may select some access restrictions as part of the online submission of this thesis. I retain all ownership rights to the copyright of the thesis. I also retain the right to use in future works (such as articles or books) all or part of this thesis.

Nicholas Louis Cuccia April 15, 2017

The Tribological Properties of Polyacrylamide Hydrogel Particles

by

Nicholas Louis Cuccia

Justin Clifford Burton

Adviser

Department of Physics

Justin Clifford Burton

Adviser

Jed Brody

Committee Member

Gillian Hue

Committee Member

2017

The Tribological Properties of Polyacrylamide Hydrogel Particles

by

Nicholas Louis Cuccia

Justin Clifford Burton

Adviser

An abstract of
a thesis submitted to the Faculty of Emory College of Arts and Sciences
of Emory University in partial fulfillment
of the requirements of the degree of
Bachelor of Sciences with Honors

Department of Physics

2017

Abstract

The Tribological Properties of Polyacrylamide Hydrogel Particles
By Nicholas Louis Cuccia

Polyacrylamide hydrogel particles are a popular material in all realms of science. In particular, they have recently become a useful system for modeling low-friction, granular materials near the jamming transition. Because a gel consists of a polymer network filled with solvent, its surface behavior exhibits non-classical tribological properties. As a result, the frictional coefficient can vary between 0.001 and 0.03 depending on several factors such as contact area, sliding velocity, normal force, and the gel surface chemistry. Previous tribological experiments of gels utilize two flat surfaces to make measurements, in which the contact area is not well defined. We have built a custom, low-force tribometer to measure the single-contact frictional properties of spherical hydrogel particles on flat hydrogel surfaces under a variety of measurement conditions. From our measurements, we have found a positive correlation between the frictional coefficient and sliding velocity and a negative correlation between the normal load and frictional coefficient. In trying to explain these results, we make use of a hydrodynamic lubrication theory for an object in Hertzian contact. Our measurements have shown that this model is accurate within the high-velocity (>1 cm/s), high-load (>0.1 N) range, but loses precision in the low-velocity (<1 cm/s) and in the low-load (<0.1 N) limit.

The Tribological Properties of Polyacrylamide Hydrogel Particles

by

Nicholas Louis Cuccia

Justin Clifford Burton

Adviser

A thesis submitted to the Faculty of Emory College of Arts and Sciences
of Emory University in partial fulfillment
of the requirements of the degree of
Bachelor of Sciences with Honors

Department of Physics

2017

Acknowledgements

I gratefully acknowledge Jed Brody and Gillian Hue for taking time out of their schedules to serve on my committee. Furthermore, I thankfully acknowledge all members of the Burton laboratory, especially Juan Jose, who first introduced me to scientific research and led me to my early path. Above all, I thank my adviser Justin Burton. This work would not exist without his outstanding mentorship. As a first-year student with litter knowledge or experience, Justin was willing to let me work with him in his laboratory. He taught me all that I know about research and helped me to find my path as a student. Every opportunity, he has helped push towards success, and I cannot thank him enough for being such a kind and caring mentor. Through the fun times to the hard times, thank you for your kindness and love.

Table of Contents

List of Figures and Tables

Introduction

Between a solid and liquid: If you have ever made Jell-O, you are fully away of its fun and silly properties. Jell-O is a squishy wet solid. You can jiggle it, wiggle it, and shake it all over, yet it will retain its form. In short, it is slippery, like a fluid, yet rigid, like a solid. Of course, this duality of softness and rigidness in not unique to Jell-O, and is, in actuality, an attribute of nearly all gels being a consequence of the fundamental structure of gels.

At the molecular scale, a gel consists of polymers, or long chain molecules, which are hooked together into a network. Like a sponge, this structure likes to absorb and retain certain solvents (such as water, alcohol, etc.). As the liquid fills the gaps between the polymers, this network is stretched and expanded out (see Figure 1). The absorbed liquid keeps the gel from collapsing into a compact mass, and the polymer network stops the liquid from flowing away.

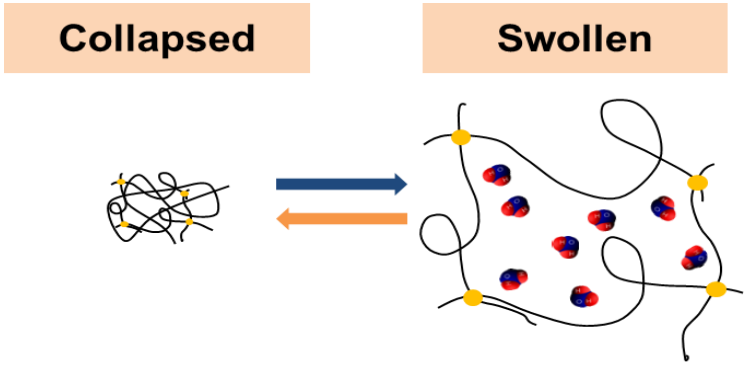

Figure 1: Schematic representation of gels in collapsed and swollen states. The solid lines and open circles denote polymer chains and crosslinking points, respectively.

The final result is a material which consists almost entirely of fluid while retaining the structure of a solid. The amount of fluid that polymer network retains is truly incredible and hard to overstate. For example, the Jell-O we make in our kitchens consists of 3% polymer network and 97% sugar water [1]. Naturally, this substance which has both structure and softness is has many useful applications throughout the different fields of science.

Gels are everywhere: It is not always immediately clear how pervasive gels are within the realms of our lives. You are likely to encounter them persistently, and it is no exaggeration to say that our world

would be drastically different without them. Throughout our day, we use them to style our hair [2], correct our vision [3], and make delicious sugary desserts [4]. Within the realm of biomedical and materials engineering, gels are used to make artificial skin layers [5], diapers [6], synthetic soil [7], and so much more [8-10]. It is truly exceptional that an object only discovered and named in the mid-1800s has now become a such a common and important item without our world.

Granular systems: In Burton Lab, we are particularly interested in applying gels to a 2-D granular system (see Figure 2). As a brief review, a granular material consists of a collection of discrete macroscopic particles, with a typical example being the sand in an hourglass or the sugar in a bowl. At first glance, a person might not expect the physics of a sand pile to be complicated. However, it has been observed that granular systems do not act in a Newtonian fashion [11-13]. Amazingly, a granular material can mimic gas, liquid, solid, plastic flow, glassy behavior, and more [14-16].

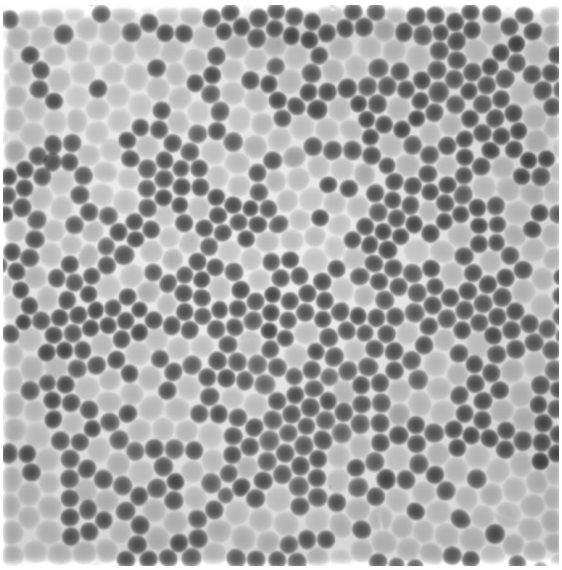

Figure 2: A jammed low-friction granular system consisting of hydrogel particles. Image curtesy of Burton Lab.

Because granular systems are so strange, there is a lot of effort within the scientific community to better understand them. In Burton Lab, we are trying to create and examine granular systems consisting of low-friction particles to better understand the role of friction within the pile's internal interactions.

When trying to select a material for our particles, gels seem to be a natural choice. They have slippery low-friction surfaces, from their large amounts of retained fluid, while still maintaining a consistent

physical shape, because of their polymer networks. For our purposes, the gel of choice has been polyacrylamide hydrogel which, as the name implies, is a gel whose absorbed solvent is water.

Strange surface properties: While gels are very useful, they are also very odd. There are bands of studies which show how gels act in non-classical ways. They have unusual volume transitions [17], mechanical instabilities [18], surface variations [19], and more [20-23].

Because of the extensive use of polyacrylamide hydrogel within our lab, we became curious about their specific physical properties. In studying our gel's surfaces, we hoped to understand potential interactions within our 2-D granular system better while contributing information to the soft matter community as a whole.

Our early experiments started with the observation of a surface instability that occurred when hydrogel was absorbing water (see Figure 3). We created imaging systems and examined the instability through a variety of external conditions. After a thorough literature review, however, we determined that the questions involving this instability have been extensively examined. Figure 4 shows just one example of the comprehensive imaging and modeling that has been achieved in recent years on this topic [23].

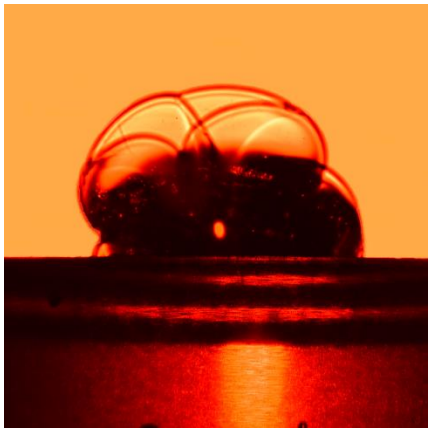

Figure 3: The surface instability of hydrogel during absorption of water.

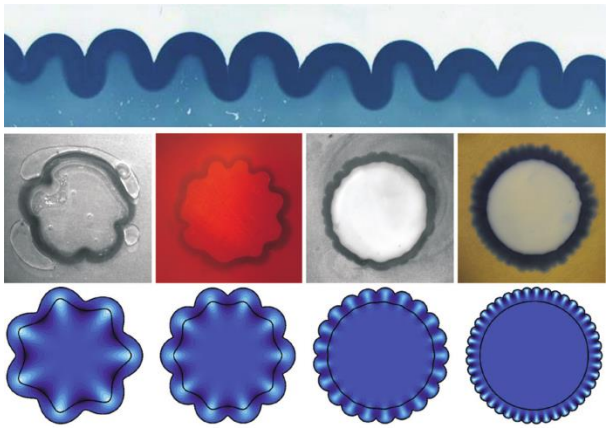

Figure 4: Buckling of a swelling gel (top) matched with corresponding theoretical predictions (bottom) [23].

From here, we chose to move onto the topic which will be the primary focus of this thesis, the surface friction of polyacrylamide hydrogel.

Strange frictional properties: Gels, in general, are known for having a low surface friction. Because they consist mostly of fluid, they are extremely slippery, being able to slide with friction coefficients as low as 10^{-3}. While several studies have looked into the specific tribological properties of gels [24-28], there remain questions about the consistency and precision of these previous experiments.

The purpose of this thesis will be to examine the frictional coefficient of our polyacrylamide hydrogel in a highly accurate and consistent manner. In accomplishing this goal, we have designed and constructed a custom high precision pin-on-disc tribometer to obtain measurements with a resolution of 0.1 mN. Using this device, we have examined the coefficient of friction under a wide range of sliding velocities and normal loads.

For this collected data, we have derived frictional relationships using existing elastohydrodynamic lubrication theories for soft materials. By comparing existing theory to our findings, we expect to be able to detect any possible polymer interactions which may be occurring within the gel-on-gel contact and determine for what situations existing lubrication theory may act as an adequate predictor of the hydrogel frictional effects.

Background

***Classical friction**:* The classical laws of friction are well-known and commonly taught within any introductory physics course [30-31]. For the purpose of this thesis, it is important to be actively aware of several properties laid out through Amontons' laws. These three rules, proposed by Amontons in 1699, represent the basis of standard tribological theory and provide important insight into the material properties of surfaces. Amontons' laws state that for a system experiencing kinetic friction (such as a block being pulled against another block):

1. The frictional force (f) is proportional to the normal load (N),

$$f \propto N. \tag{1}$$

2. The frictional force *does not* depend on the contact area (A) between the two surfaces.
3. The frictional force *does not* depend on the sliding velocity (U) of the two surfaces.

This theory also defines the coefficient of friction (μ) as the dimensionless constant of proportionality between the frictional force and the normal load in Eq. 1.

In simple classical systems, the coefficient of friction is a deterministic value set by the material properties of the objects being rubbed together. It does not depend on any external factors, such as sliding velocity or contact area, and is inherent to the system itself.

Gel Friction: It is a widely-observed fact [24-28] that two gel surfaces rubbed together do not follow the classical laws set out by Amontons. Instead, the frictional properties of gels are dependent on their sliding velocity [24], contact area [25], normal load [26], and surface chemistry [27]. Over the last two decades, many researchers have been trying to find the exact relationship between the coefficient of friction and these four factors.

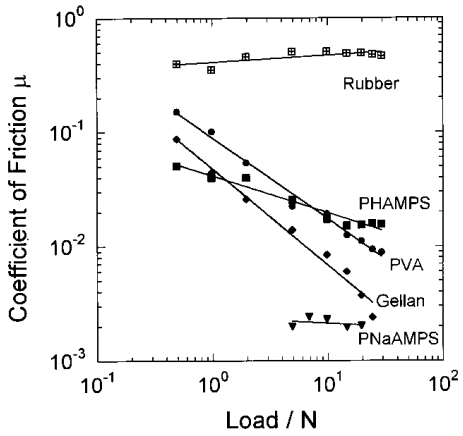

Figure 5: Coefficients of friction for different gels at differing normal loads (sliding velocity of 7 mm/min). [26]

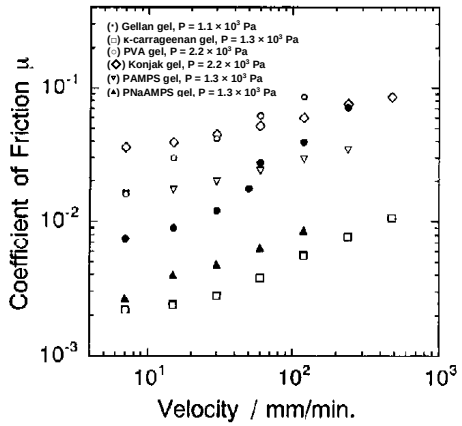

Figure 6: Coefficients of friction for different gels at differing sliding velocities. [24]

From existing literature, we can examine the frictional dependencies that exist within several different gels. Figures 5 and 6, for example, show the coefficients of friction for a range of gels across different sliding velocities and normal loads.

These charts reveal several important details, the most striking of which is that the coefficient of friction is negatively correlated with load. This is so important that it is worth emphasizing, *the higher the normal load, the lower the coefficient of friction* [26]. As far as classical tribology is concerned, no material has this kind of property, and it is certainly not an intuitive result.

Another point of interest is that the relationship between the coefficient of friction and sliding velocity (and normal load) depends entirely on which chemical gel is used [26-28]. This emphasizes how the surface chemistry can affect the coefficient of friction.

As of this existing moment, these previous studies have not yet studied the surface properties of polyacrylamide hydrogel (our preferred gel). As such, there is no certainty as to what frictional relations may be found because of our experiment. We do, however, hope to see trends similar to what has previously been found.

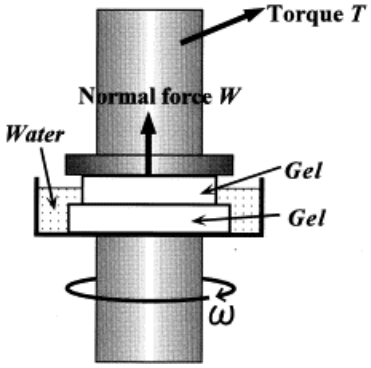

Figure 7: Tribometer spinning two discs of gel against each other to measure frictional forces. [26]

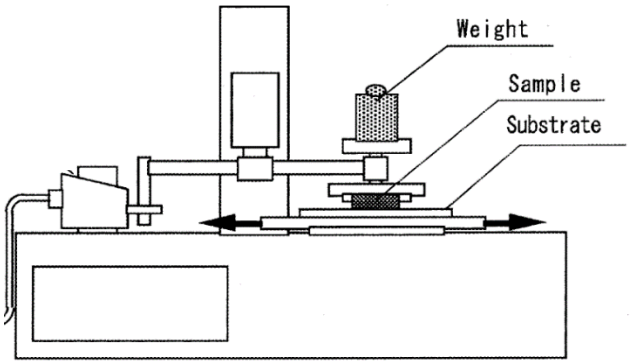

Figure 8: Tribometer pulling two slabs of gel sliding against each other to measure frictional forces. [26]

Tribological Methods: Perhaps the most distinguishing aspect of our experiment is that it deviates from previous literature regarding the approach used to examine the tribological properties of gels. So far, in previous studies, there have been two primary methods implemented in determining a gel's frictional coefficient. The first involves rotating two gel discs against each other and measuring the resistive torque (see Figure 7) [26]. The second involves pulling two slabs of gel against each other, and measuring the resistive force (see Figure 8) [26].

In recent years, there have arisen questions about the precision of these tribological methods for examining gels [29]. In particular, researchers have found that the large gel surfaces utilized in previous experiments can lead to uneven pressure pockets between the surfaces (see Figure 9).

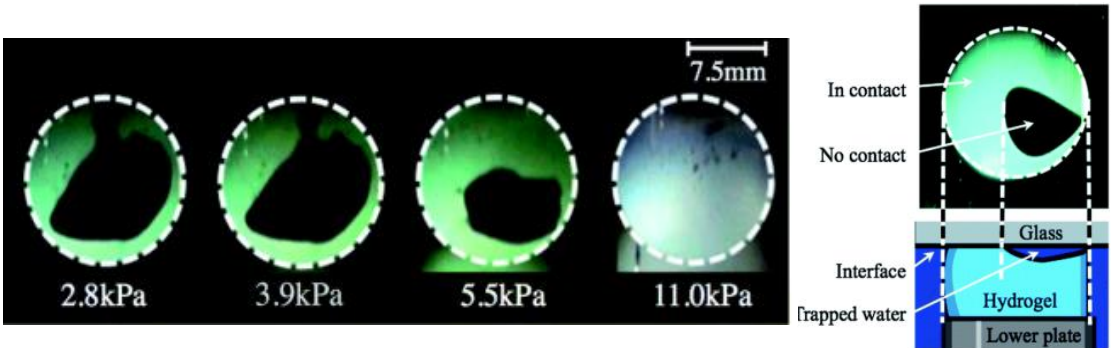

Figure 9: The hydrogel forms a heterogeneous contact with the adhesive surface, causing a water drop to be trapped at the interface. [29]

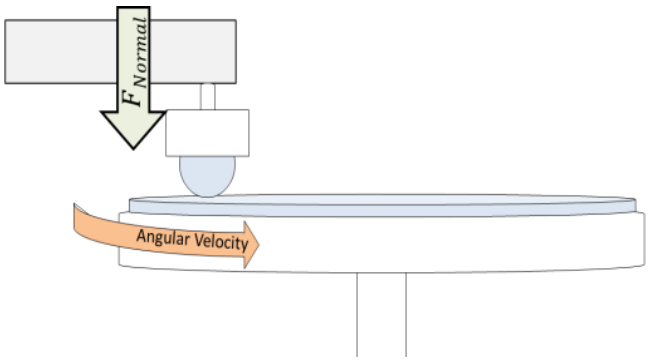

Figure 10: Example of a pin-on-disc tribological setup.

These heterogeneous pockets make it difficult to accurately define our gel's contact area (which the frictional coefficient is dependent on) and can cause inconsistent results. Because these pressure pockets exist within the range of normal loads used for most friction experiments, it is hard to be confident in the accuracy of previous experiments.

In this thesis, we attempt to tackle this problem by creating a more precise experimental setup. Instead of using two slabs of gel against each other, we chose to pursue a gel sphere on a gel disc, known as a pin on disc model (see Figure 10). This setup allows us to minimize the contact area between the gels, and prevent any heterogeneous pressure pockets.

Lubrication layer: In classical tribological theory, we have two *dry-solid-surfaces* drag against each other. Of course, many more configurations can exist beyond just a dry solid surface. For example, you can introduce a fluid into your system creating a combination of two *wet-solid-surfaces*.

When examining the contact between two gels, the existence of some form of fluid layer can be clearly seen [29]. This is, of course, not surprising as a gel consists of close to 97% fluid. In

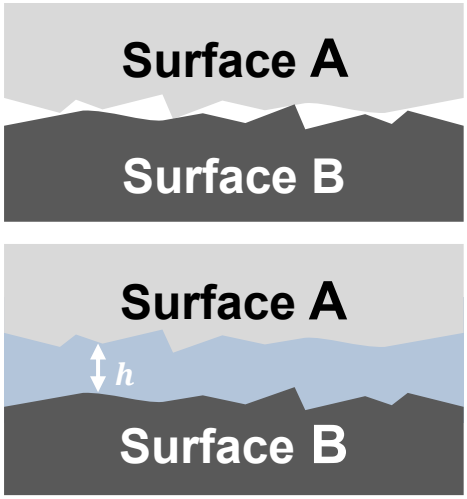

Figure 11: Example of a dry contact (top) and a lubricated contact (bottom). The thickness of the lubrication layer is denoted h.

essence, two gels in contact will have a liquid lubrication layer between them.

Naturally, the introduction of fluid between two surfaces substantially changes the tribological theory for the system. Instead of having two surfaces rubbing against each other, we now have a liquid rubbing against two surfaces (see Figure 11).

For these kinds of situations, it becomes necessary to know information about the fluid *and* the surfaces. We must now have knowledge of variables such as the thickness and viscosity of the liquid layer in order to adequately describe the viscous drag (friction force) that occurs on our surfaces.

Elasto-Hydrodynamic Model: At this point, we want to try and create a model for how the frictional coefficient should scale with velocity and normal force in our experimental system. To determine these relations, we will make use of elastohydrodynamic theory involving a lubricated contact between two soft elastic bodies [32-34].

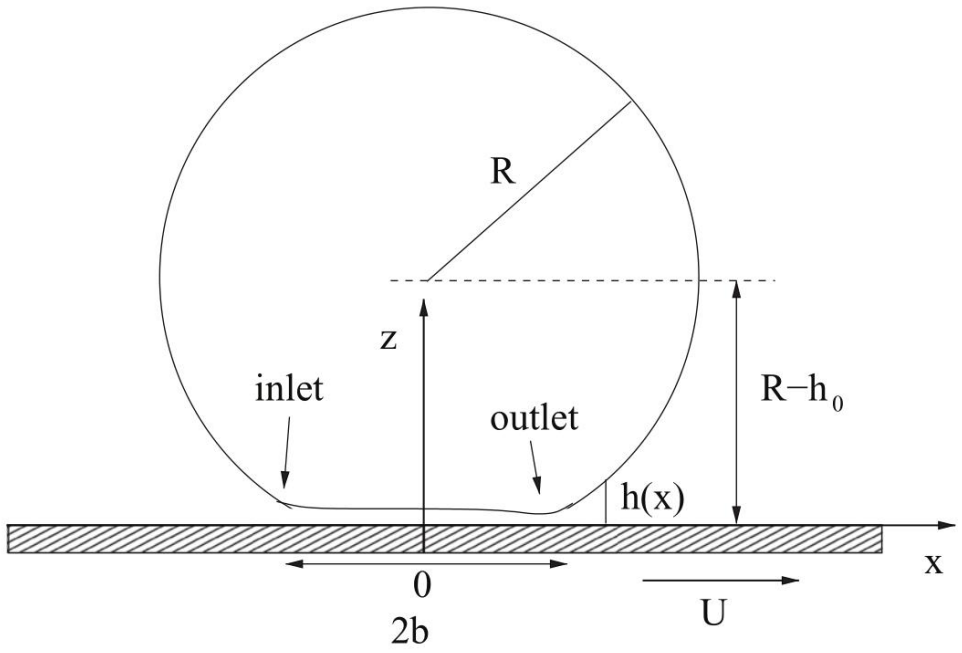

Figure 12: A 2-D side profile of an infinite elastic cylinder in lubricated contact with an infinite plane. The cylinder is experiencing a large enough load to have flat elastic deformation at its base. [33]

In this model, there exists an infinite soft cylinder of radius R and an infinite soft plane which are in lubricated contact (see Figure 12). The two bodies are moving with a relative speed U to each other, and there is a normal load per unit length L exerted downwards on the cylinder.

For our derivation, we are only using normal loads which are large enough to create a Hertzian contact between our surfaces. In other words, the normal load is sufficiently significant to cause the deformation on the bottom of the cylinder to be nearly flat (see Figure 12). This has the consequence of making the lubrication layer uniform in thickness between the plane and cylinder.

Our goal, at this point, is to determine an equation which defines the thickness of the lubrication layer. Thankfully, this problem has already been solved with the height of the lubrication layer (denoted h_{gap}) determined using partial-differential similarity theory [33]. The exact solution is,

$$h_{gap} = H^* \left[2\pi (3\eta U R)^3 \frac{(1-\sigma^2)^2}{LY^2} \right]^{1/5}. \tag{2}$$

Here η is the viscosity of the fluid in the lubrication layer, L is a normal load per unit length, Y is the young's modulus of the cylinder, σ is the Poisson ratio of our material (typically ~ 0.5), and $H^* = 0.4467$ is a unique universal inlet solution for the similarity equations.

While Eq. 2 was derived using an infinite cylinder, it has also been shown to be valid in the case of a finite soft sphere in Hertzian contact within a deformable plane [33], which is significantly closer to our experimental setup. In this new situation, Figure 12 could just be viewed as a cross-section through the center of a sphere, instead of a slice of a cylinder.

When using Eq. 2 for a sphere, we will need to make a minor modification, as the load per unit length L is not well-defined for a finite sphere. Instead, we will want to make use of the ordinary normal load N, which we do by making the substitution,

$$L = \frac{N}{2b}. \tag{3}$$

Here $2b$ is the width of the flat contact between a cylinder and its fluid layer (or the diameter of the circular contact between a sphere and its fluid layer).

From Hertzian contact theory, we are able to define the value of b for a sphere in terms of its normal load, radius, Poisson ratio, and young's modulus. The relation comes out to be:

$$b = \left[3NR\frac{(1-\sigma^2)}{4Y}\right]^{1/3}. \tag{4}$$

We can now substitute Eq. 3 and Eq. 4 into Eq. 2 to obtain our final relation for the lubrication thickness,

$$h_{gap} = H^*\left[\frac{[48]^{1/3}\pi R^{10/3}(3\eta U)^3(1-\sigma^2)^{5/3}}{N^{2/3}Y^{5/3}}\right]^{1/5}. \tag{5}$$

Because of the complicated nature of lubrication mechanics, it can be difficult to tell if Eq. 5 seems reasonable. Thankfully, however, this result has been experimentally tested (see Figure 13) and shown to be accurate [34].

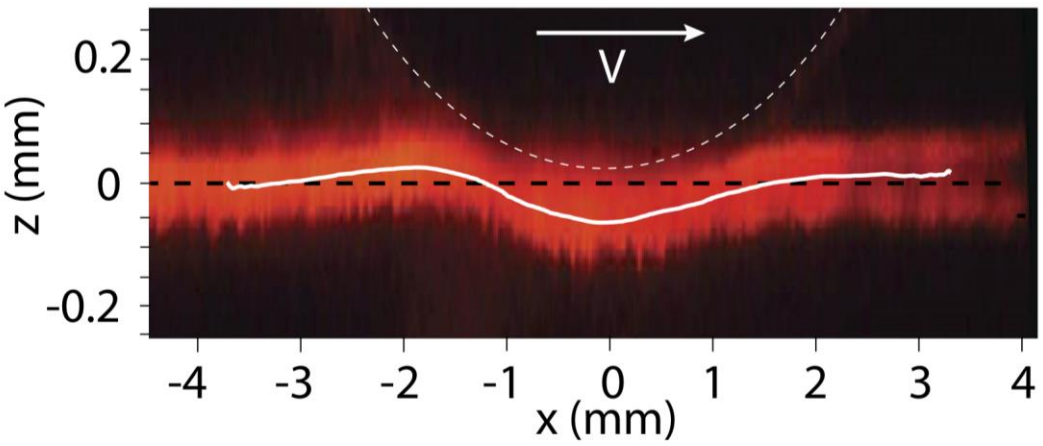

Figure 13: Experimental verification of Eq. 5. This experiment made use of a cylinder on a plane format, similar to Figure 12. The gap thickness was found to closely fit the theoretical predictions [34].

Since we are primarily interested in the lubrication thickness' proportionality to sliding velocity and normal load, it is helpful to re-write Eq. 5 as,

$$h_{gap} \propto U^{3/5} N^{-2/15} . \tag{6}$$

Now that we have the thickness of the lubrication layer, it is a simple task to determine the drag force (frictional force) exerted on our sphere. We can start with the equation [35] for the drag force D as,

$$D = \int_0^b \eta U \frac{4h(x) - 3d}{h(x)^2} \, 2\pi r \, dr. \tag{7}$$

Here, the lubrication layer's height at any given point is defined as $h(x)$ and the layer's overall effective height is defined as d. Because we are in Hertzian contact, the lubrication layer is assumed to be uniform in height, and so $h(x) = d = h_{gap}$. Hence, we can re-write Eq. 7 as,

$$D = \int_0^b 2\pi r \eta \, U \frac{1}{h_{gap}} dr = \pi \eta U \frac{b^2}{h_{gap}} . \tag{8}$$

At this point, we are mainly interested in how D depends on velocity and normal load. As such, we will drop the constant coefficients and focus only on the proportionality of Eq. 8. Using Eq. 4 and Eq. 6, we can find that,

$$D \propto U^{2/5} N^{4/5}. \tag{9}$$

Finally, we can divide Eq. 9 by the normal load to obtain our coefficient of friction,

$$\mu = \frac{D}{N} \propto U^{2/5} N^{-1/5}. \tag{10}$$

With Eq. 10, we now have a prediction for how the frictional coefficient will scale to velocity and normal load. Interestingly, Eq. 9 has a negative correlation with normal load, matching the observations of previous gel studies [26].

Materials and Methods

Ultra-Low Friction Tribometer: As mentioned before, one of the primary goals of this experiment has been to design and use a tribometer that allows for precise and consistent measurements. The optimal way to achieve this goal was through the utilization of a pin-on-disc tribological method. In designing this kind of apparatus, we wanted to create a simple manner to:

1. Vary the sliding velocities
2. Vary the normal loads
3. Obtain extremely high-resolution measurements

With these technical constraints, we found the optimal design was through the use of a lever-arm style apparatus that connected to a force sensor (see Figure 14). This device allows for the easy addition and removal of masses, letting us carefully control the normal loads applied to our gels. On the base of the tribometer, we switched between two voltage variable DC motors (a high-velocity and low-velocity model), which allowed for exact control of the sliding velocity through an external voltage generator.

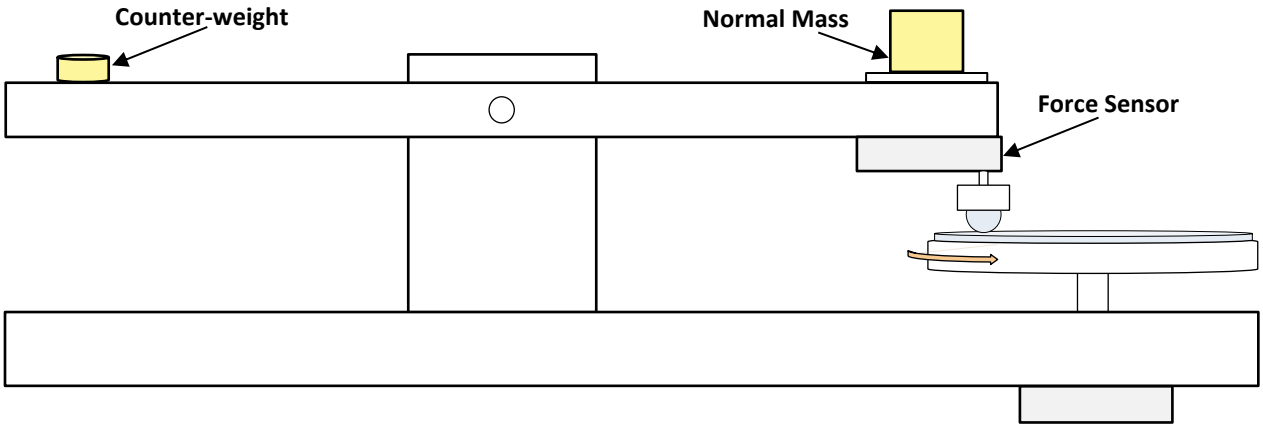

Figure 14: A side view of our tribological setup. We used a pin-on-disc model, creating an extremely consistent and precise experiment. We used an S256 10g Force Sensor from Strain Measurement Devices, and two (a low and high velocity) Compact Square-Face DC Gearmotors from McMaster-Carr.

In order to obtain the needed resolution in our measurements of the frictional coefficients, which can be as small as 10^{-3}, we utilized an S256 10g Force Sensor from Strain Measurement Devices. This device has a resolution of 0.1 mN, allowing us to clearly see any variations in the frictional coefficients that may occur.

The force sensor was connected to our computer by wiring it through an NI USB-6525 data acquisition device (DAQ) from National Instruments. Data was collected through the LabView software which controlled and managed the DAQ.

Polyacrylamide Hydrogel: One of the primary obstacles of this experiment was obtaining a hydrogel disc to use within our tribometer. Unfortunately, such an item is not easily purchasable. As such, we created a complete manufacturing setup, allowing us to mix the necessary chemicals to obtain polyacrylamide hydrogel. Our resulting hydrogels consisted of a 29:1 acrylamide to bis-acrylamide mixture.

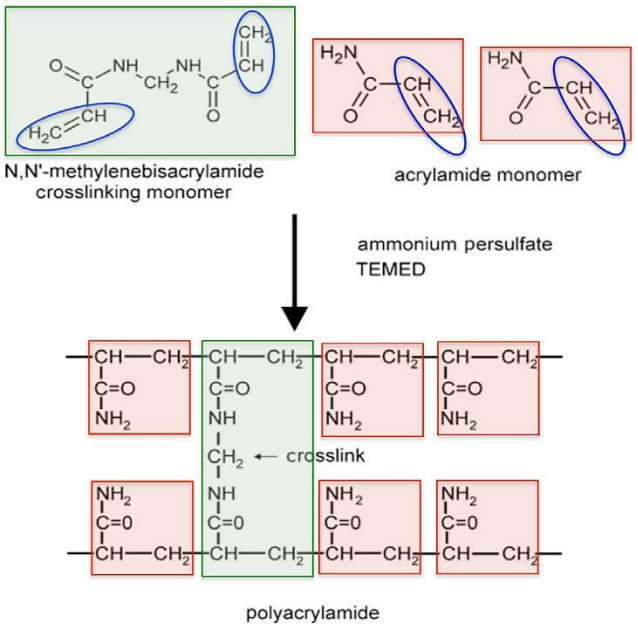

Figure 15: A chemical diagram of the polymerization process between acrylamide (a monomer) and bis-acrylamide (a crosslinking monomer) [36].

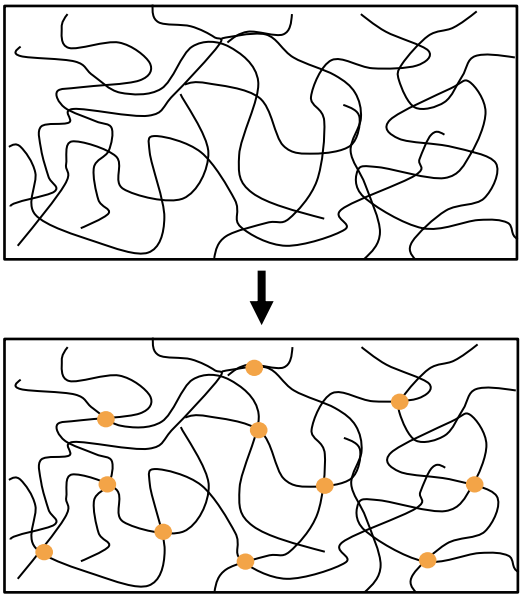

Figure 16: A chemical diagram of the crosslinking of individual polymers. The solid circles are crosslinked points.

We make use of a free-radical polymerization process which creates polyacrylamide hydrogels by a copolymerization of acrylamide and bis-acrylamide [36]. We initially prepare a solution of acrylamide and bis-acrylamide monomers. Then we add a mixture of ammonium persulfate and TEMED (tetramethylethylenediamine), which releases free radicals into the monomer solution and starts the polymerization process (See Figure 15).

As the acrylamide monomers interact with the free-radical particles, they become activated, allowing them to initiate the polymerization process by hooking onto other acrylamide monomers into a long chain (polymer). As these long acrylamide chains come into existence, they are randomly crosslinked to each other by a monomer of bis-acrylamide (see Figure 16), resulting in a polyacrylamide hydrogel.

Because this polymerization process is random, it can create inconsistent and uneven surfaces on our gels. This can often lead to difficulties since our experiment is so dependent on the geometric configuration of our gels. Hence, it is imperative to remedy this issue.

We resolved this problem by crosslinking our hydrogel within an acrylic mold. The mold causes the gel to form into a smooth and uniform shape, in this case, a disc. A mold also has the benefit of allowing us to control the exact dimensions of our gels. By laser-cutting our containers out of acrylic, we were able to obtain a gel disc of diameter and thickness needed.

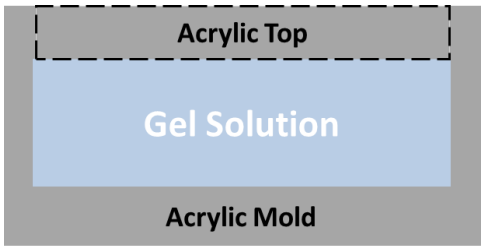

Figure 17: Acrylic gel mold which allows gel solutions to polymerize into smooth consistent discs.

Results and Discussion

Coefficient vs. Sliding Velocity: Now with our experimental setup in hand, and theoretical models derived, we are ready to obtain and examine the coefficients of friction for our gels. We start with a simple situation in which we apply a load of 0.2N to our gel and measure the frictional coefficient while varying the sliding velocity.

In Figure 18, each trial uses a different gel particle within the tribometer. Trials 1 and 2 make use of the same gel disc, whereas Trial 3 uses a different disc. In all three trials, the chemical structure of the gel spheres and discs are kept consistent, respectively.

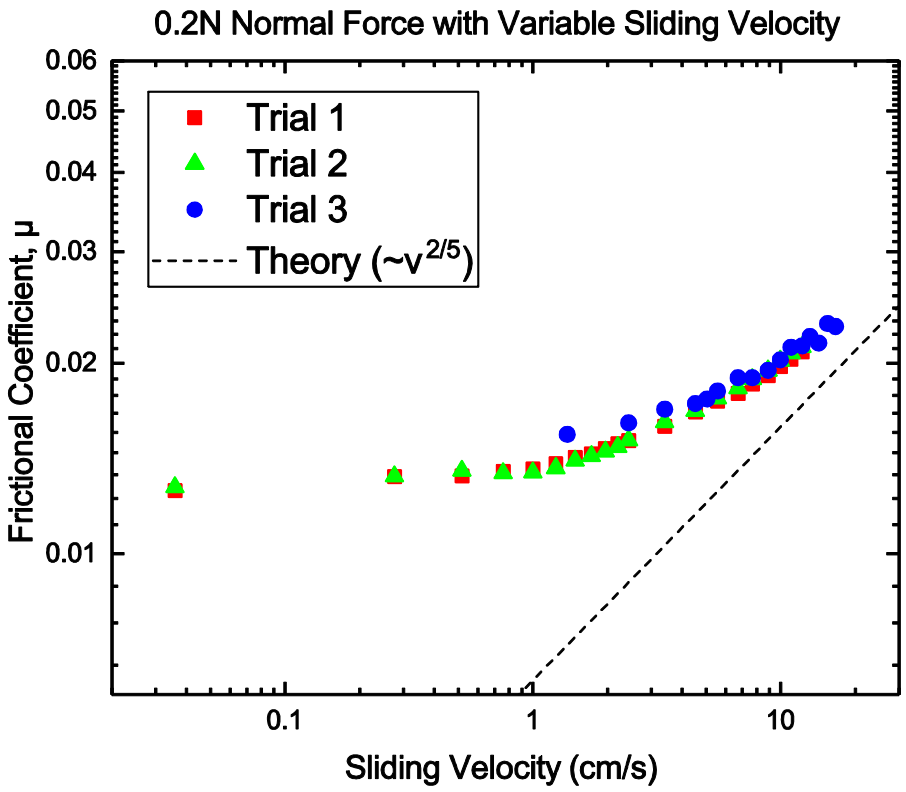

Figure 18: Measurement of the frictional coefficient across a range of sliding velocities for three different gel particles across two gel discs. Our data trends towards the theory at higher sliding velocities. Note that trial 3 doesn't have measurements below 1 cm/s.

As we can see in Figure 18, our measurements are consistent across several trials and are small in magnitude (around 10^{-2}). Interestingly, our results overshoot the elastohydrodynamic theory, but trend towards it at higher velocities. Particularly, our high-velocity results seem to be off by some constant cofactor. At lower velocities, the theory falls apart and is no longer predictive of the frictional coefficients for our gels. It is also interesting that our coefficient appears to trend to some constant value as we approach a zero velocity, which also doesn't match our theoretical predications.

It seems that there may be some polymer-network interactions occurring between the gels that are not considered by our theoretical model. There appears to be some transition around 5 cm/s at which these polymer interactions could be becoming a dominant influence.

Coefficient vs. Normal Load: Our next choice of variation is the normal load. We choose to examine the frictional coefficients at a range of loads between 0.1 N and 0.4 N across the same range of velocities as our previous measurements in Figure 18.

In Figure 19, each normal load data set uses two different gel particles, all on the same disc. We average the measurements to obtain the results seen on the curve.

In Figure 19, we observe several significant trends. First, we notice the negative correlation between the frictional coefficient and normal load. As we increase the mass pushing on the gel, the coefficient of friction clearly decreases. This fits our theoretical prediction and the findings of previous experiments. This matches our theoretical prediction, and the results of previous studies.

Another striking feature of our graph are the distances between the four curves. At high normal loads, we see little difference in our frictional coefficients. The values for the 0.3 N data set are nearly identical to the values for the 0.4 N dataset. Whereas, for small normal loads, there are huge differences between 0.1 N data set and the 0.2 N dataset.

We notice that a similar trend seems to present itself within our theoretical values. The gap between the 0.1 N theory curve and the 0.2N theory curve is larger than that of the 0.3 N curve and the 0.4 N curve. However, the distances between the predicted values do appear smaller than the distances between our measured results.

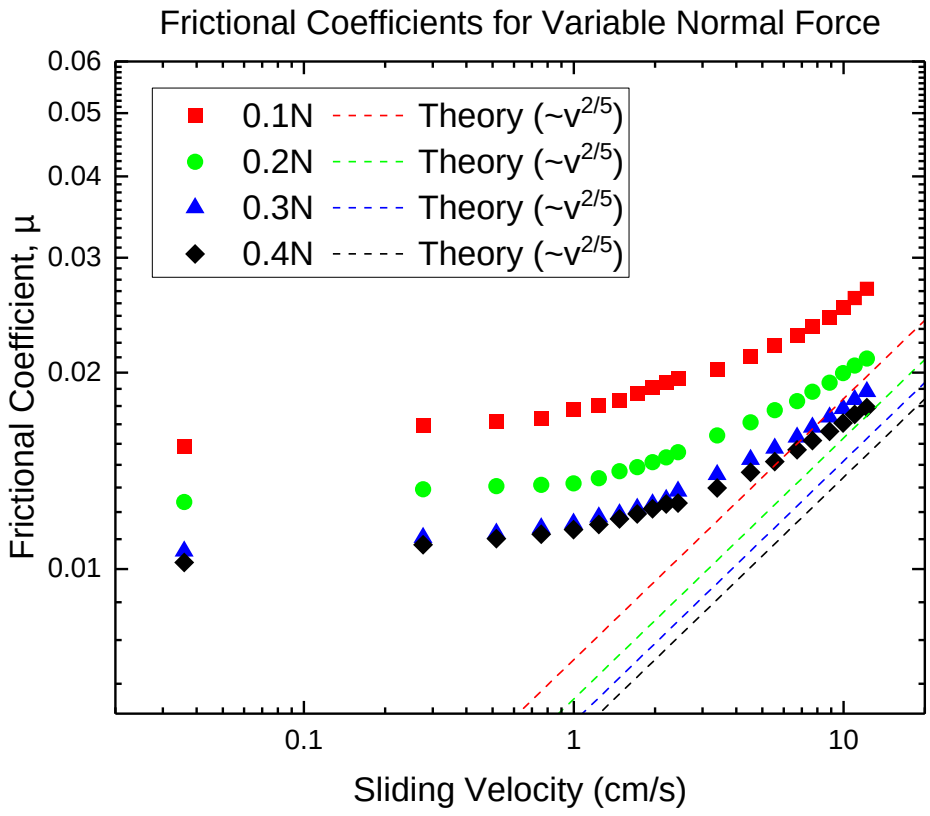

Figure 19: Measurement of the frictional coefficient across a range of sliding velocities for four different normal loads. Each set of data consists of measurements for two different particles on the same gel disc that are averaged together. Our data trends towards the theory at higher sliding velocities.

Normalization of Curves: In order to get a better idea about the difference between the theoretical values and the experimental values in Figure 19, we are going to normalize the data sets using Eq. 10. If this experiment perfectly matched the theory, then this adjustment would have the effect of collapsing all our data atop each other.

Instead, what Figure 20 shows is that the experimental values collapse for higher normal loads, but not for lower normal loads. It can also be seen that the overlap becomes more significant at the higher velocities, indicating that our theoretical prediction is more accurate for higher velocities.

The normal load dependence could be explained by Hertzian contact theory. Potentially, a force of 0.1 N is not large enough to maintain a good Hertzian contact, thus causing a heterogeneous lubrication

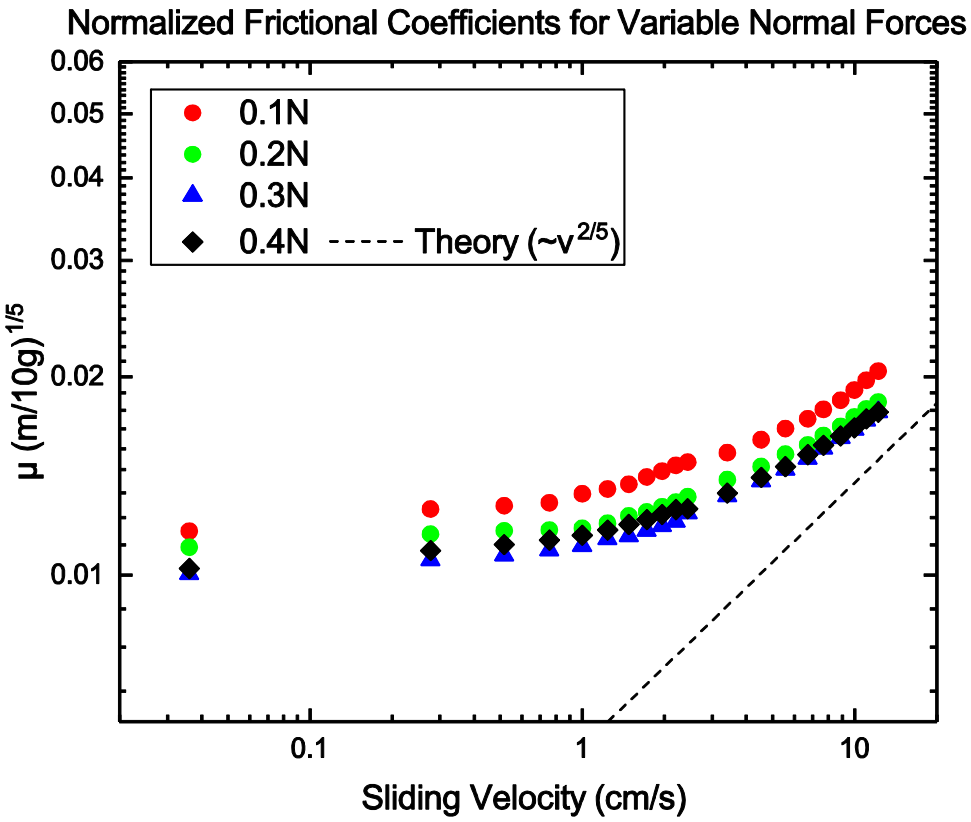

Figure 20: Normalization of Figure 19 by normal load. While the theoretical curves collapse onto each other, the experimental curves show a distinct spread. We see clearly that our theoretical relation between frictional coefficient and normal load does not match the experimental measurements.

layer. If this were the case, then our theoretical model would be inadequate in the low-mass limit, hence the deviation for our data. An alternative possibility is that there may be some unexpected polymer-polymer interactions that we are not considering. However, it is not clear if this is the case.

A Solid Ball: In order to get a better idea of any possible polymer interactions occurring within our system, we chose to replace our gel sphere with a hard metal ball.

As Figure 21 shows, the metal ball nearly returns us to the realm of classical tribological theory. Rather than have a coefficient of friction which varies with velocity, we witness a fairly constant value for the metal ball. This emphasizes that the frictional effects between our gel surfaces are not just caused by the existence of a fluid layer, but by some other unaccouunted polymer interaction.

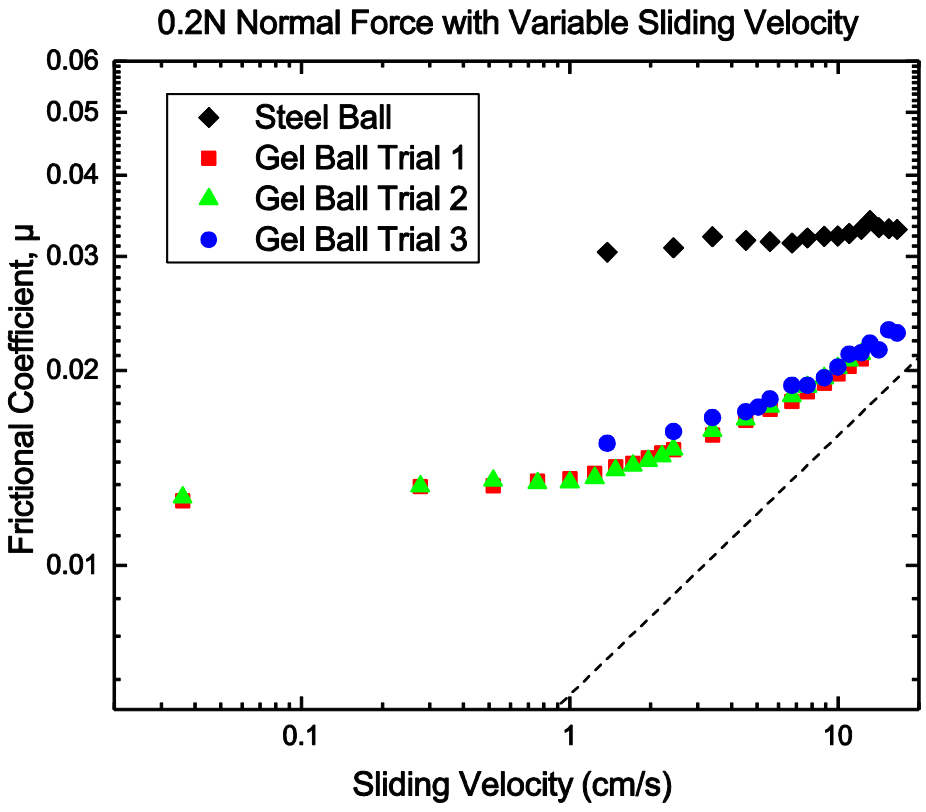

Figure 21: Examination of coefficient of friction for a hard steel ball against as gel disc. We see a clear distinction between the tribological properties of the metal ball as compared to that of the gel sphere.

Final Remarks

Conclusions: Over the course of two years, we have designed and built a custom pin-on-disc tribometer, which has allowed us to examine gel friction in a low-contact limit. Through the utilization of an ultra-low force sensor, with a resolution of 0.1 mN, we have been able to clearly see any fluctuations in the frictional coefficient over a range of normal loads and sliding velocities.

From our measurements, we have shown a positive correlation between the frictional coefficient and sliding velocity, and a negative correlation between the normal load and frictional coefficient, similar to that found in previous literature.

In the high-velocity, high-force limit, we see a trend towards our theoretical prediction. However, in the low-velocity and low-force limits, we see a large deviation from our proposed soft elasto-lubrication model. This indicates that there is some further interaction that is not being taken into account by our model.

Future Directions: We intend to obtain more knowledge about the exact mechanical and surface properties of our hydrogel. Because the elastic modulus is important within our theoretical description of our system, we plan to fully measure this value for our gel disc and our gel sphere.

In a similar vein, we also intend to explicitly image the contact between our gel sphere and our gel disc to better see if Hertzian contact is being maintained and if the contact varies largely for different normal loads.

Finally, we aim to examine the frictional coefficient over an even larger range of sliding velocities in order to see if our measurements will approach our theoretical values at higher velocities.

References

1 Tanaka, T. (1981). Gels. *Scientific American*, 244(1), 124–138.

2 Jain, J., Arora, S., Rajwade, J. M., Omray, P., Khandelwal, S., & Paknikar, K. M. (2009). Silver nanoparticles in therapeutics: development of an antimicrobial gel formulation for topical use. *Molecular Pharmaceutics*, *6*(5), 1388-1401. 10.1021/mp900056g

3 Ahmed, E. M. (2015). Hydrogel: Preparation, characterization, and applications: A review. *Journal of Advanced Research*, *6*(2), 105-121. 10.1016/j.jare.2013.07.006

4 Banerjee, S., & Bhattacharya, S. (2012). Food gels: gelling process and new applications. *Critical reviews in food science and nutrition*, 52(4), 334-346. 10.1080/10408398.2010.500234

5 West, J. L., & Hubbell, J. A. (1995). Photopolymerized hydrogel materials for drug delivery applications. *Reactive Polymers*, *25*(2), 139-147. 10.1016/0923-1137(94)00096-N

6 Kozak, T. F. (1975). *U.S. Patent No. 3,890,974*. Washington, DC: U.S. Patent and Trademark Office.

7 Hüttermann, A., Zommorodi, M., & Reise, K. (1999). Addition of hydrogels to soil for prolonging the survival of Pinus halepensis seedlings subjected to drought. *Soil and Tillage Research*, *50*(3), 295-304. 10.1016/S0167-1987(99)00023-9

8 Deligkaris, K., Tadele, T. S., Olthuis, W., & van den Berg, A. (2010). Hydrogel-based devices for biomedical applications. *Sensors and Actuators B: Chemical*, 147(2), 765-774. 10.1016/j.snb.2010.03.083

9 Beebe, D. J., Moore, J. S., Bauer, J. M., Yu, Q., Liu, R. H., Devadoss, C., & Jo, B. H. (2000). Functional hydrogel structures for autonomous flow control inside microfluidic channels. *Nature*, *404*(6778), 588-590. 10.1038/35007047

10 Cortese, R., & Theeuwes, F. (1982). *U.S. Patent No. 4,327,725*. Washington, DC: U.S. Patent and Trademark Office.

11 Kadanoff, L. P. (1999). Built upon sand: Theoretical ideas inspired by granular flows. Reviews of Modern Physics, 71(1), 435. 10.1103/RevModPhys.71.435

12 Fournier, Z., Geromichalos, D., Herminghaus, S., Kohonen, M. M., Mugele, F., Scheel, M., ... & Skudelny, A. (2005). Mechanical properties of wet granular materials. *Journal of Physics: Condensed Matter*, *17*(9), S477. 10.1088/0953-8984/17/9/013

13 Liu, A. J., & Nagel, S. R. (1998). Nonlinear Dynamics: Jamming is not just cool any more. *Nature*, *396*(6706), 21–22. 10.1038/23819

14 Savage, S. B. (1984). The mechanics of rapid granular flows. *Advances in applied mechanics*, *24*, 289-366. 10.1016/S0065-2156(08)70047-4

15 Liu, A. J., & Nagel, S. R. (2010). The Jamming Transition and the Marginally Jammed Solid. *Annual Review of Condensed Matter Physics*, *1*(1), 347–369. 10.1146/annurev-conmatphys-070909-104045

16 Weeks, E. R., Crocker, J. C., Levitt, A. C., Schofield, A., & Weitz, D. A. (2000). Three-dimensional direct imaging of structural relaxation near the colloidal glass transition. *Science*, *287*(5453), 627-631. 10.1126/science.287.5453.627

17 Tanaka, T., Nishio, I., Sun, S.-T., & Ueno-Nishio, S. (1982). Collapse of Gels in an Electric Field. *Science*, *218*(4571), 467–469. 10.1126/science.218.4571.467

18 Dervaux, J., & Amar, M. Ben. (2012). Mechanical Instabilities of Gels. *Annual Review of Condensed Matter Physics*, *3*(1), 311–332. 10.1146/annurev-conmatphys-062910-140436

19 Scott, R. P., & Kucera, P. (1978). Solute-solvent interactions on the surface of silica gel. *Journal of Chromatography A*, *149*, 93-110

20 Tanaka, Y., Gong, J. P., & Osada, Y. (2005). Novel hydrogels with excellent mechanical performance. *Progress in Polymer Science*, *30*(1), 1–9. 10.1016/j.progpolymsci.2004.11.003

21 Seiffert, S. (2015). *Supramolecular Polymer Networks and Gels*. (S. Seiffert, Ed.) (1st ed., Vol. 268). Cham: Springer International Publishing. 10.1007/978-3-319-15404-6

22 Suzuki, A., & Tanaka, T. (1990). Phase transition in polymer gels induced by visible light. *Nature*, *346*(6282), 345–347. 10.1038/346345a0

23 Dervaux, J., Couder, Y., Guedeau-Boudeville, M. A., & Ben Amar, M. (2011). Shape transition in artificial tumors: From smooth buckles to singular creases. *Physical Review Letters*, *107*(1), 1–4. 10.1103/PhysRevLett.107.018103

24 Kagata, G., Gong, J. P., & Osada, Y. (2002). Friction of Gels. 6. Effects of Sliding Velocity and Viscoelastic Responses of the Network. *The Journal of Physical Chemistry B*, *106*(18), 4596–4601. 10.1021/jp012380w

25 Yashima, S., Takase, N., Kurokawa, T., & Gong, J. P. (2014). Friction of hydrogels with controlled surface roughness on solid flat substrates. *Soft Matter*, *10*(18), 3192–9. 10.1039/c3sm52883a

26 Gong, J., Higa, M., Iwasaki, Y., Katsuyama, Y., & Osada, Y. (1997). Friction of Gels. *The Journal of Physical Chemistry B*, *101*(97), 5487–5489. 10.1021/jp9713118

27 Kagata, G., Gong, J. P., & Osada, Y. (2003). Friction of Gels. 7. Observation of Static Friction between Like-Charged Gels. *The Journal of Physical Chemistry B*, *107*(37), 10221–10225. 10.1021/jp022463s

28 Gong, J. P., Iwasaki, Y., Osada, Y., Kurihara, K., & Hamai, Y. (1999). Friction of Gels. 4. Friction on Charged Gels. *The Journal of Physical Chemistry B*, *103*, 6007–6014. 10.1021/jp990256v

29 Yamamoto, T., Kurokawa, T., Ahmed, J., Kamita, G., Yashima, S., Furukawa, Y., … Gong, J. P. (2014). In situ observation of a hydrogel-glass interface during sliding friction. *Soft Matter*, *10*, 5589–96. 10.1039/c4sm00338a

30 Hutchings, I. M., & Shipway, P. (1992). Tribology: friction and wear of engineering materials. 10.1243/PIME_PROC_1993_207_110_02

31 Tipler, P. A., & Mosca, G. (2007). *Physics for scientists and engineers*. Macmillan.

32 Pandey, A., Karpitschka, S., Venner, C. H., & Snoeijer, J. H. (2016). Lubrication of soft viscoelastic solids. *Journal of Fluid Mechanics*, *799*, 433–447. 10.1017/jfm.2016.375

33 Snoeijer, J. H., Eggers, J., & Venner, C. H. (2013). Similarity theory of lubricated Hertzian contacts. *Physics of Fluids*, *25*(10). 10.1063/1.4826981

34 Jules, T., Salez, T., & Mahadevan, L. (2016). Correction for Saintyves et al., Self-sustained lift and low friction via soft lubrication. *Proceedings of the National Academy of Sciences*, *113*(50), E8208–E8208. 10.1073/pnas.1616995113

35 Fallis, A. . (2013). *Physics of Continuous matter*. *Journal of Chemical Information and Modeling* (Vol. 53). 10.1017/CBO9781107415324.004

36 Menter, P. (2000). Acrylamide Polymerization—A Practical Approach. *Bio-Rad Tech Note*, 1156.